



## A CROSS-POLARIZER METASURFACE DESIGN FOR K- AND KA-BAND APPLICATION STUDIES

Abdulkadir ÇILDIR<sup>1\*</sup>

<sup>1</sup> Elektrik Elektronik Mühendisliği, Mühendislik Mimarlık Fakültesi, Mehmet Akif Ersoy Üniversitesi, Burdur, 15030, Türkiye,

Keywords	Abstract
<i>Metasurface, Cross-Polarizer, PCR, Angular Stability, Broadband.</i>	In this study, a novel cross-polarizer metasurface (CPM) is presented. The metasurface is designed on Roger 5880 substrate by using CST microwave studio. The metasurface design features a split-ring that incorporates a U-shape. This metasurface can convert an $x/y$ -polarized linear incident wave into a $y/x$ -polarized linear wave in K- and Ka- frequency bands. It has a bandwidth of 12.15 GHz (11.95–12.6 GHz, 23.5–35 GHz) with an efficiency of 90% polarization conversion ratio (PCR). This design also has angular stability up to 30 degrees. This study comes in handy with some K- and K-band application studies.

## K VE KA-BANT UYGULAMA ÇALIŞMALARI İÇİN ÇAPRAZ POLARİZE EDİCİ METAYÜZEY TASARIMI

Anahtar Kelimeler	Öz
<i>Metayüzey, Çapraz Polarize Çevirici, PCR, Açısız Kararlılık, Geniş Bant.</i>	Bu çalışmada, yeni bir çapraz kutupsal metayüzey (CPM) sunulmuştur. Metayüzey, CST mikrodalga stüdyosu kullanılarak Roger 5880 alt tabakası üzerinde tasarlanmıştır. Metayüzey tasarımı, U şeklini içeren bölünmüş bir halka içerir. Bu metayüzey, K ve Ka frekans bantlarında $x/y$ kutupsal bir doğrusal dalgayı $y/x$ kutupsal doğrusal bir dalgaya dönüştürebilir. 12.15 GHz geniş bantta (11.95-12.6, 23.5-35 GHz) %90 kutupsal dönüşüm oranına (PCR) sahiptir. Bu tasarım ayrıca 30 dereceye kadar açısız kararlılığa sahiptir. Bu çalışma, bazı K- ve Ka-bant uygulama çalışmalarında kullanışlıdır.

### Alıntı / Cite

Çıldır, A., (2025). A cross-polarizer metasurface design for K- and Ka-band application studies, Mühendislik Bilimleri ve Tasarım Dergisi, 13(2), 613-622.

### Yazar Kimliği / Author ID (ORCID Number)

A. Çıldır, 0000-0003-1789-6088

### Makale Süreci / Article Process

<b>Başvuru Tarihi / Submission Date</b>	13.08.2024
<b>Revizyon Tarihi / Revision Date</b>	06.05.2025
<b>Kabul Tarihi / Accepted Date</b>	06.05.2025
<b>Yayın Tarihi / Published Date</b>	27.06.2025

\* İlgili yazar / Corresponding author: acildir@mehmetakif.edu.tr, +90-248-213-28-03

## A CROSS-POLARIZER METASURFACE DESIGN FOR K- AND KA-BAND APPLICATION STUDIES

Abdulkadir ÇILDIR<sup>1†</sup>

<sup>1</sup> Electrical Electronics Engineering, Faculty of Engineering and Architecture, Mehmet Akif Ersoy University, Burdur, 15030, Türkiye, acildir@mehmetakif.edu.tr

---

### Highlights

---

- It transforms polarizations.
  - It works in K and Ka application studies.
  - It converts x/y- linear polarized wave to y/x- linear polarized wave.
  - It has a good PCR (polarization conversion ratio).
  - It has an angular stability up to 30 degrees.
- 

### Purpose and Scope

To design a metasurface which transforms linear polarized wave to another linear polarized wave.

### Design/methodology/approach

The unit cell is designed on a Roger 5880 substrate with a thickness of 1.6 mm, a loss tangent of 0.025, and a permittivity of 4.3. The presented unit cell is composed of a split ring including U-shape. A metallic ground supports the unit cell. This design works in K and Ka application studies. It works as a cross-polarizer which can transform a polarized wave to another. It has a 90% polarization conversion ratio (PCR) efficiency in the 12.15 GHz broadband (11.95-12.6, 23.5-35 GHz). This design also has angular stability up to 30 degrees.

### Findings

The reflection coefficient results are shown for x- and y- polarized waves. As seen in these graphs, the same results are given for two different polarized waves. These same results result from the mirror image of the unit cell in xy-orthogonal axis. Co-reflection coefficient results should be as low as possible to obtain a CPC, while cross-reflection coefficients should be equal. Polarization conversion ratio (PCR) results are given for normal and oblique incidence waves, respectively. These results show that this design has linear-to-linear conversion over 90% efficiency across 11.95-12.6, 23.5-35.0 GHz for normal incidence wave and also efficiently performs linear-to-linear conversion up to 30 degrees.

### Originality

This paper has a new design with a high PCR value. This paper works in a broadband including K and Ka band. It has also an angular stability up to 30 degrees.

---

<sup>†</sup> Corrospounding Author: acildir@mehmetakif.edu.tr, +90-248-213-28-03

## 1. Introduction

Metasurfaces are two-dimensional arrays of subwavelength unit cell structures. These structures have been suggested for numerous applications, including polarization manipulation, incident wave absorption (Amin, Fida et al. 2022), antenna gain enhancement (Samantaray and Bhattacharyya 2020, Nasser and Chen 2021), electromagnetic wave diffusion (Al-Nuaimi, He et al. 2019), flexible beam formation using (Wu, Hou et al. 2023), satellite applications (Shukoor, Dey et al. 2022), EMC applications (Chandra, Samantaray et al. 2022), and radar cross-section reduction (Liu, Li et al. 2021). If metasurface structures are anisotropic, they can be utilized in cross-polarization conversion (CPC), where linear polarization (LP) plays a crucial role.

Polarization defines the direction of the electric field in an electromagnetic wave. The electric field can oscillate in different types of polarization such as linear, circular, and elliptical, which are used in different areas. However, in some applications such as antenna systems (Wang, Shao et al. 2022), optical instruments (Bi, Huang et al. 2022, Ullah, Zhao et al. 2022), medical imaging (Razzicchia, Ghavami et al. 2023), communication systems (Zhang, Sun et al. 2022, Yang, Zheng et al. 2023), it is important to convert one polarization to another. Metasurfaces are one of the materials, which can transform the polarization states of electromagnetic waves. Metasurfaces are able to be called cross-polarizers if they make linear-to-linear (LTL) conversion.

Recently, various designs for LTL have been proposed. These include arrow-shaped structures (Rashid, Murtaza et al. 2023), split ring resonators (SRR) developed by (Wahidi, Khan et al. 2020), (Kamal, Chen et al. 2021). Additionally, Z-shaped structures (Wang and Zhai 2020) and chessboard structures (Al-Nuaimi, Hong et al. 2019) have been investigated. The main objectives of these designs are to achieve broadband linear polarization (LP) (Cildir, Tahir et al. 2024), high polarization conversion ratio (PCR), low axial ratio, and high angular stability (Çildir 2024). Meanwhile, to enhance the total bandwidth, various studies (Zhao, Qi et al. 2019, Kamal, Chen et al. 2021, Liu, Li et al. 2021, Chandra, Samantaray et al. 2022, Shukoor, Dey et al. 2022, Xu, Gao et al. 2022) have reported bandwidths of 20.64, 9.5, 10.2, and 5.1 GHz, respectively, for LTL conversion in reflection mode.

It is seen from the given studies, broadband and angular stability of metasurfaces are still insufficiently addressed in the literature. This paper presents a new metasurface a split ring cross-polarizer metasurface (SR-CPM) that stands out for its versatility, wide frequency coverage, and straightforward design. The device features unit cells on one side and a full copper layer on the other. It can conduct both LTL conversion efficiency greater than 90% over a frequency band ranging from 11.95-12.6, 23.5-35 GHz. It can also LTL conversion at different oblique angles up to 30 degrees. The research is proposed into segments that delve into unit cell design, polarization theory, simulation results and discussions, and conclusion.

## 2. Material and Method

The designed unit cell configuration for a metasurface is shown in Fig. 1. The unit cell is designed on a Roger 5880 substrate with a thickness of 1.6 mm, a loss tangent of 0.025, and a permittivity of 4.3. The dimensions of the unit cell, shown in Fig. 1, is determined using the optimization feature of CST Microwave Studio using Periodic boundary conditions with Floquet ports. The presented unit cell is composed of a split ring including U-shape. A metallic ground supports the unit cell.

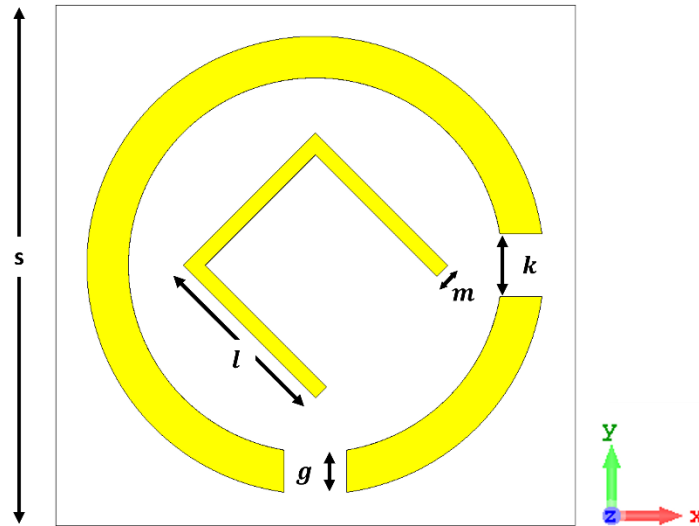


Fig. 1. Designed unit cell with its dimensions ( $s: 7, k: 1.2, l: 1.8, m: 0.15, g: 0.4$ )

For electromagnetic waves which are coming towards  $z$ -direction,  $x$ -polarized incident electromagnetic wave to the metasurface, they are reflected as  $y$ -polarized electromagnetic waves. If  $y$ -polarized waves impinge to this metasurface, they are reflected as  $x$ -polarized waves. So, this unitcell has been designed to convert linear polarized waves to other linear polarized waves.

The incident wave into the metasurface surface is reflected by changing its polarization. This polarization conversion can be expressed with reflection coefficients. In this study, reflection coefficients, which are the ratio of the incident and reflected waves, are expressed as follows:  $R_{xx}=E_{rx}/E_{ix}$ ,  $R_{yy}=E_{ry}/E_{iy}$ ,  $R_{yx}=E_{ry}/E_{ix}$  and  $R_{xy}=E_{rx}/E_{iy}$ . Here,  $R_{xx}$ ,  $R_{yy}$  are co-reflection coefficients and  $R_{yx}$ ,  $R_{xy}$  are cross-reflection coefficients.

In Fig. 2, the reflection coefficient results are shown for  $x$ - and  $y$ -polarized waves. As seen in these graphs, the same results are given for two different polarized waves. These same results result from the mirror image of the unit cell in  $xy$ -orthogonal axis. Co-reflection coefficient results should be as low as possible to obtain CPC, while cross-reflection coefficients should be equal. In Fig. 2 is seen that co-reflection coefficients results are below threshold value ( $-10$  dB) in some frequency regions ( $11.95$ - $12.6$  GHz,  $23.5$ - $35$  GHz), while cross-reflection coefficient results are about  $0$  dB.

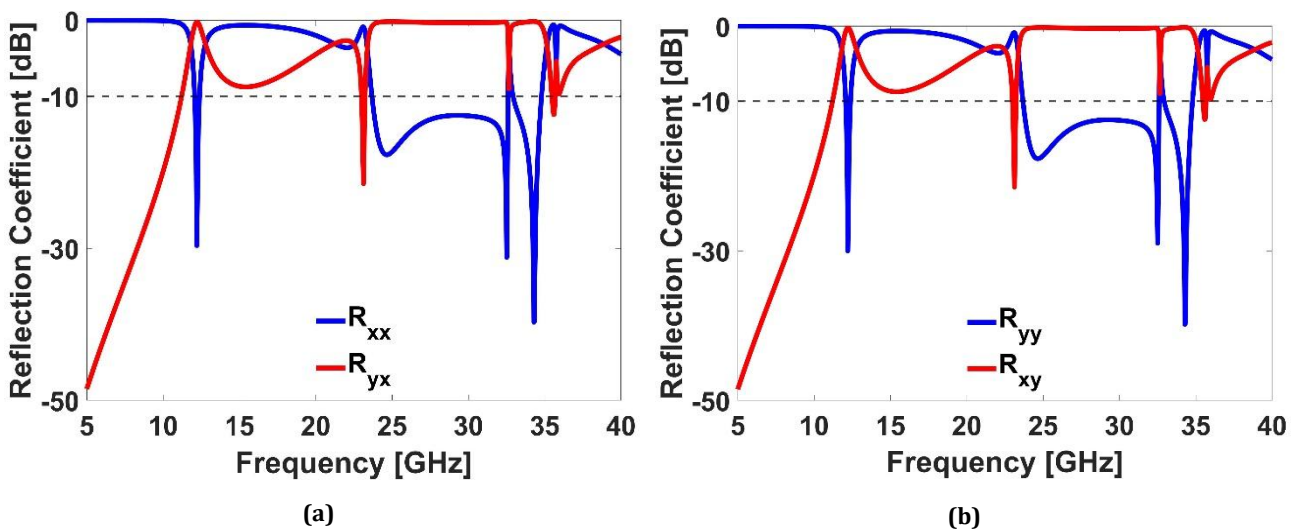


Fig. 2. Reflection coefficient simulation results for (a)  $x$ -, (b)  $y$ - polarized incident waves.

In Fig. 3, the designed unit cell is shown on the  $uv$ - axis. This axis helps us understand more cross polarization conversion existence. This axis is obtained  $xy$ - axis by rotating 45 degrees in horizontal plane. Equ. (1) and (2) analyze the electric field components on this axis in Fig. 3.

$$\mathbf{E}_{iy} = \hat{y}E_i = \vec{u}E_{iu}e^{j\varphi_{iu}} + \vec{v}E_{iv}e^{j\varphi_{iv}} \quad (1)$$

$$\mathbf{E}_{rx} = \hat{x}E_r = \vec{u}E_{ru}e^{j\varphi_{ru}} + \vec{v}E_{rv}e^{j\varphi_{rv}} \quad (2)$$

Here, the components  $E_{iy}$  and  $E_{rx}$  can be expressed in terms of components  $E_{iu}$ ,  $E_{iv}$ ,  $E_{ru}$ , and  $E_{rv}$  as described in Equ. (2) and (3). In this context, '  $\varphi$  ' expresses the phase of the wave, while the subscripts '  $i$  ' and '  $r$  ' refer the incident and reflected waves, respectively. The subscripts '  $y, x, u, v$  ' indicate the directions of the waves.

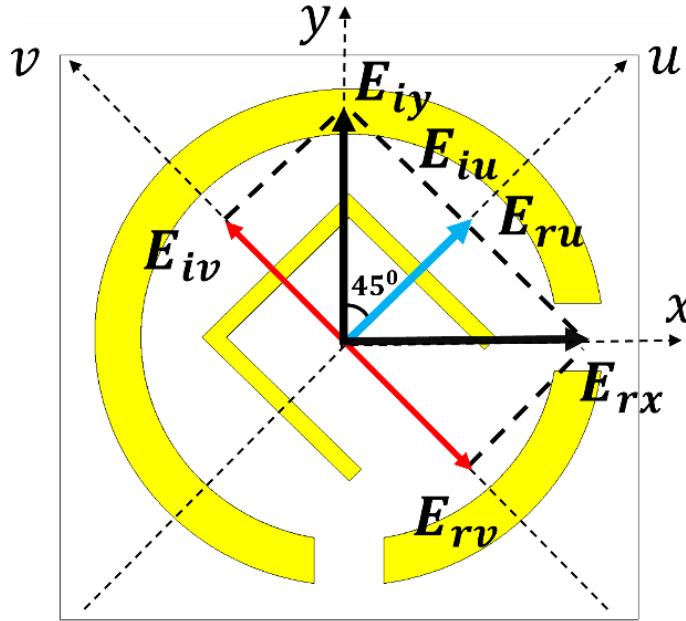


Fig. 3. Unit cell design on the  $uv$ - axis

For this unit cell, reflection coefficients  $R_{uu}=E_{ru}/E_{iu}$  and  $R_{vv}=E_{rv}/E_{iv}$  can write on the  $uv$ - axis. When  $R_{uu}$  and  $R_{vv}$  are placed in Equ. (1) and (2), it is seen that the equal circumstances  $|R_{uu}| = |R_{vv}| \cong 0 \text{ dB}$  and  $\Delta\varphi = \varphi_{uu} - \varphi_{vv} \cong \pm\pi$  must be ensured to obtain CPC.

### 3. Results and Discussion

In Fig. 4, reflection coefficient results are presented for the unit cell on the  $uv$ - axis. Fig. 4 (a) and (b) illustrate  $R_{uu}$  and  $R_{vv}$  and their phase difference. Analyzing Fig. 4 (a) and (b) using the mentioned equations reveals that the magnitudes of  $R_{uu}$  and  $R_{vv}$  are approximately equal and 0 dB within the working frequencies of the unit cell. Additionally, the phase difference between  $R_{uu}$  and  $R_{vv}$  follows a  $\pm 180$ -degree line. These results indicate that the designed unit cell can transform an  $x/y$ -incident wave into a  $y/x$ -reflected wave.

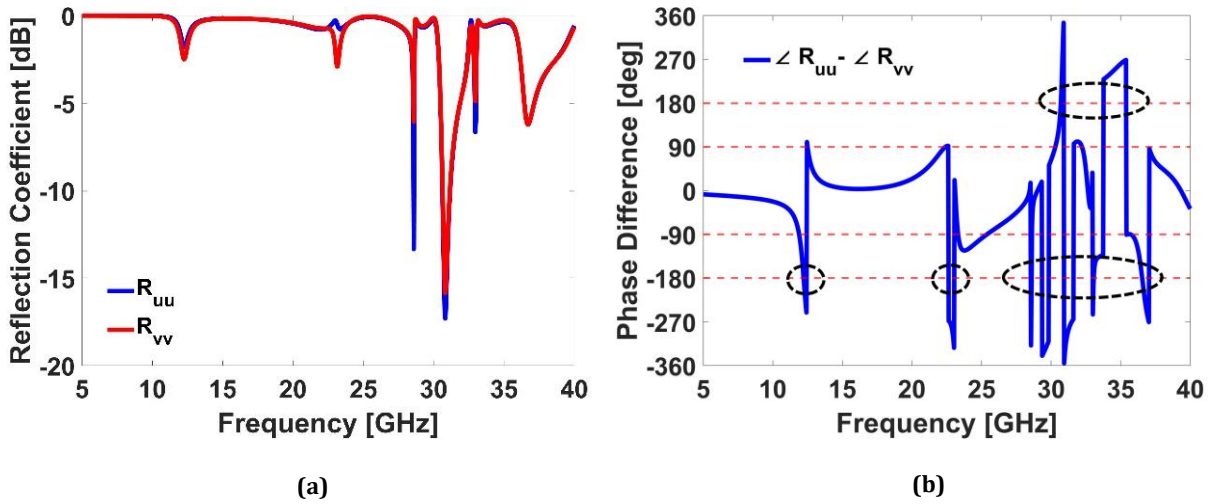


Fig. 4. (a) Reflection coefficient results, (b) reflection coefficient phase differences, on the uv- axis

In Fig. 5, polarization conversion ratio (PCR) results are given for normal and oblique incidence waves, respectively. PCR is an efficiency ratio for CPC and can be expressed as follows:

$$PCR = \frac{|R_{xy}|^2}{|R_{xy}|^2 + |R_{yy}|^2} \times 100 \quad (3)$$

In Fig. 5 (a), frequency points showing 90% efficiency have been signed. Fig. 5 (a), this design can make linear conversion over 90% efficiency across 11.95-12.6, 23.5-35.0 GHz, for normal incidence wave.

Fig. 5 (b) shows PCR results for oblique incidences. As seen in Fig. 5 (b), in the first frequency region (11.95-12.6), no change can be seen up to 30 degrees. In the other frequency region (23.5-35.0), some different frequencies come out with different angles. By seeing these results, the desing metasurface has angular stability up to 30 degrees.

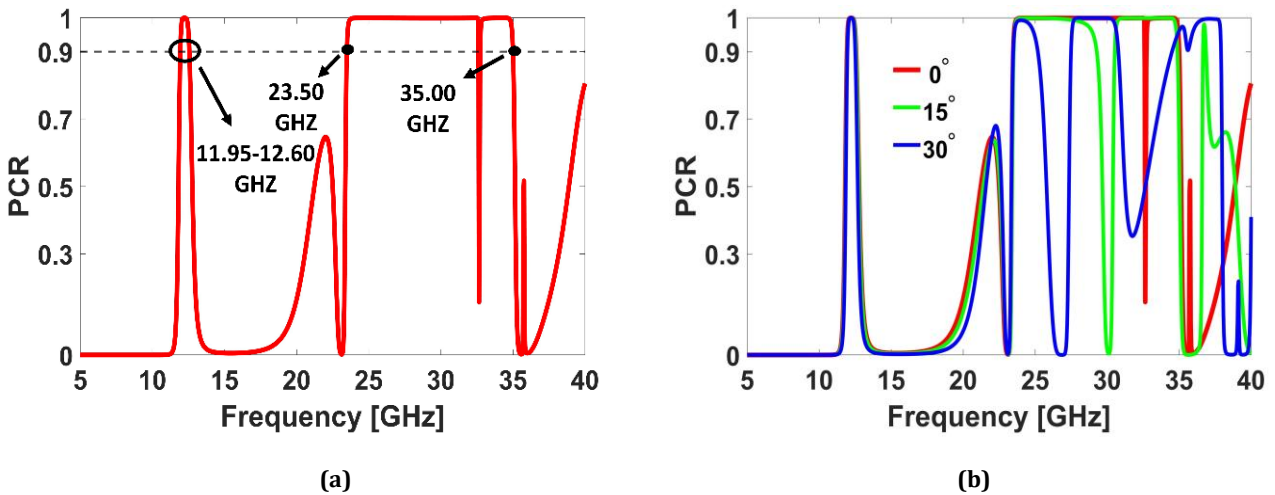


Fig. 5. PCR results for (a) normal incidence, (b) oblique incidences

The surface current distributions on the metasurface are illustrated in Fig. 6, where surface currents (a) and (c) correspond to 12.45 GHz, and surface currents (b) and (d) represent the resonance frequency of 29.25 GHz. In Fig. 6, (a) and (b) show the surface currents on the top side of the metasurface, while (c) and (d) illustrate the surface currents on the bottom side. However, the ring structure indicates the presence of a magnetic field, as the opposing surface current distribution shown in Fig. 6 confirms the existence of a magnetic field on the metasurface.

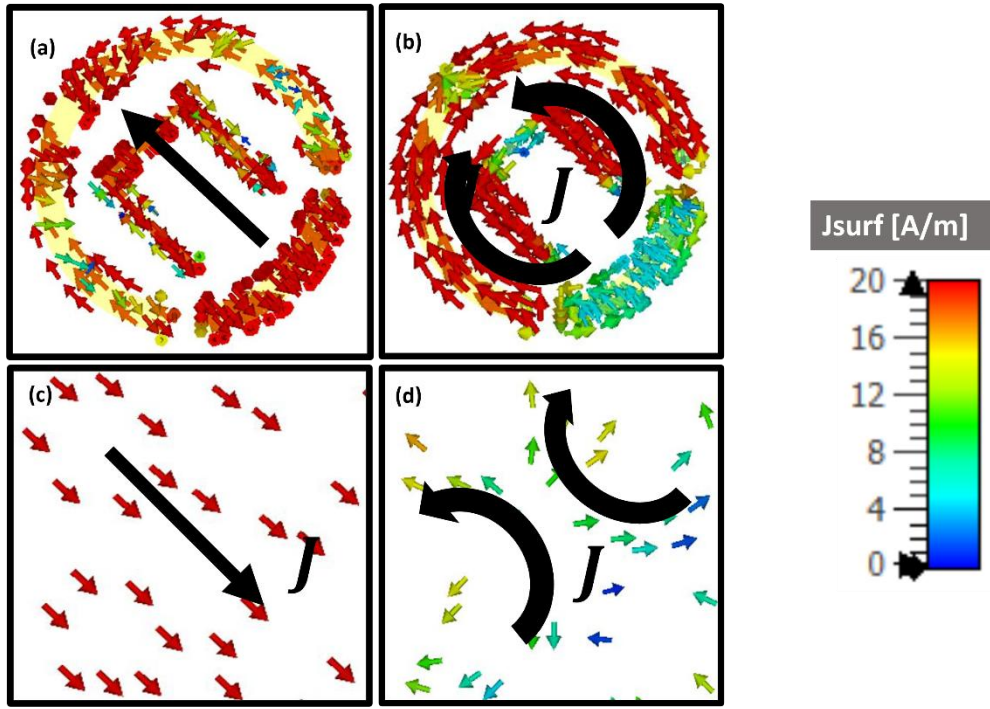


Fig. 6. Surface currents for linearly polarization at 12.45, 29.25 GHz

In the existence of the magnetic field plays crucial role the incident wave, impinging to the metasurface induces the surface currents that arise magnetic dipole moments oriented perpendicular to the metasurface. This magnetic field indicates the formation of a magnetic dipole, which contributes to the magnetic resonances responsible for the broadband behavior of the metasurface. This physical phenomenon are given in Equ. (4) and (5). (Khan, Fraz et al. 2017).

$$\begin{bmatrix} J \\ M \end{bmatrix} = i\omega \begin{bmatrix} \alpha_{ee} & \alpha_{em} \\ \alpha_{me} & \alpha_{mm} \end{bmatrix} \begin{bmatrix} E \\ H \end{bmatrix} \quad (4)$$

$$\begin{bmatrix} p \\ m \end{bmatrix} = \begin{bmatrix} \alpha_{ee} & \alpha_{em} \\ \alpha_{me} & \alpha_{mm} \end{bmatrix} \begin{bmatrix} E \\ H \end{bmatrix} \quad (5)$$

Here,  $J$  and  $M$  are electric and magnetic surface current densities, respectively.  $\omega$  is the angular frequency of the incident wave.  $\alpha_{ee}, \alpha_{em}, \alpha_{em}, \alpha_{em}$  are electric and magnetic polarizabilities of particles on the metasurface.  $E$  and  $H$  electric and magnetic field at the metasurface.

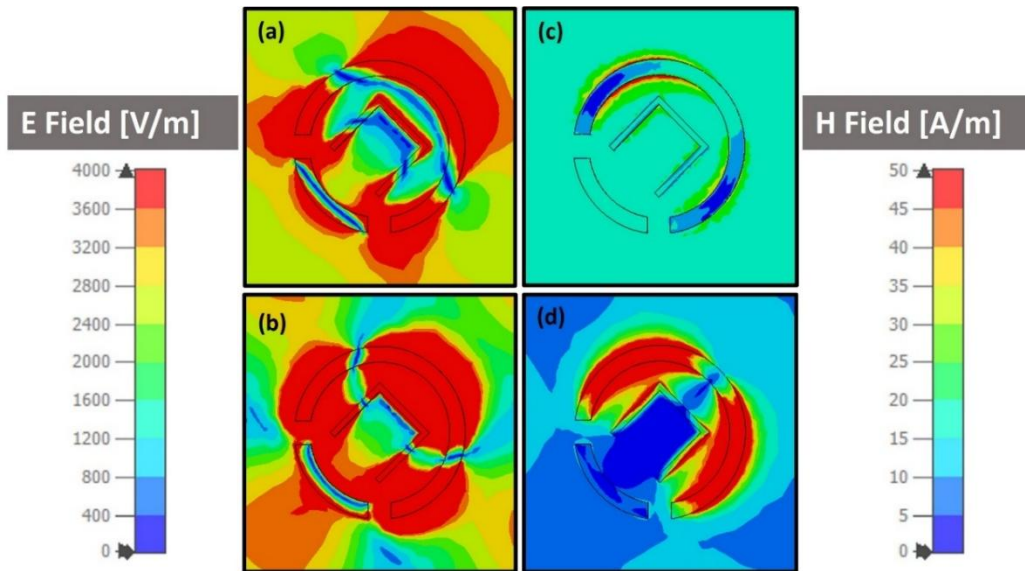


Fig. 7. E-field distributions at (a) 12.45, (b) 29.25 GHz; H-field distributions at (c) 12.45, (d) 29.25 GHz

In Fig. 7, the E-field and H-field distributions are shown on the surface of the metasurface at 12.45 and 29.25 GHz. In Fig. 7(a) and 7(b), the electric field distributions are enclosed within the C-shaped structure. In Fig. 7(c) and 7(d), the magnetic fields are more concentrated on the C-shaped side. All field distributions exhibit a diagonal pattern in Fig. 7. As a result, the different positions of the electric and magnetic responses correspond to different resonance frequencies.

Table 1. Literature comparisons

Ref.	Operation Type	Conversion Type	Frequency Band Region (GHz)	Total Bandwidth (GHz) with PCR (90%)	Angular Stability
[1] (Liu, Zhou et al. 2022)	Reflection	LTC	29-41.5 52.5-61.5	21	45
[2] (Shah, Shoaib et al. 2021)	Transmission	LTC	5.18-5.23 10.64-10.82 12.25-12.47 14.42-14.67	0.75	45
[3] (Agrahari, Rajbhar et al. 2023)	Reflection	LTL LTC	10.3-15.26 ----- 8.97-9.75 17.51-23.93	4.97 7.2	-
[4] (Qiu, Fang et al. 2023)	Reflection	LTL	6-9	3	-
[5] (Chandra, Samantaray et al. 2022)	Reflection	LTL	4.6-10.8	10.2	-
[6] (Xu, Gao et al. 2022)	Reflection	LTL	9.2-18.7	9.5	75
<b>This Study</b>	<b>Reflection</b>	<b>LTL</b>	<b>11.95-12.6 23.5-35.0</b>	<b>12.15 (90)</b>	<b>30</b>

Table 1 compares the literature studies in terms of the metasurface process type, conversion type, frequency band region, total bandwidth and angular stability. In this table, it is seen that studies 3, 4, and 5 don't have any angular stability. As study 1 operates in the higher band according to this study. It has a wider bandwidth. However, this study outperforms studies 2, 3, 4, 5, and 6 in terms of total bandwidth. It is understood from Table 1, this designed metasurface study can efficiently reflect linear polarized waves by rotating 90° and will take its place in the literature.

#### 4. Conclusion

This research introduces a novel cross-polarizer metasurface operating in reflection mode. In this paper, a split ring including U-shaped has been designed as a unit cell. Roger 5880 substrate with a thickness of 1.6 mm has been used in the design. This design achieves over 90% efficiency in converting a linearly polarized wave (x, y) into another linear polarized wave (y, x) within the frequency ranges of 11.95-12.6 GHz and 23.5-35 GHz. Additionally, this metasurface maintains angular stability up to 30°. It can be applied in linear polarization conversion for K- and Ka- bands.

#### Conflict of Interest

No conflict of interest was declared by the authors.

#### References

- Agrahari, R., et al. (2023). "Metasurface assisted wideband multifunctional polarizer." *Journal of Applied Physics* 133(9).
- Al-Nuaimi, M. K. T., et al. (2019). "Design of inhomogeneous all-dielectric electromagnetic-wave diffusive reflectarray metasurface." *IEEE Antennas Wireless Propagation Letters* 18(4): 732-736.
- Al-Nuaimi, M. K. T., et al. (2019). "Design of diffusive modified chessboard metasurface." *IEEE Antennas Wireless Propagation Letters* 18(8): 1621-1625.
- Amin, M., et al. (2022). "Anti-reflecting metasurface for broadband polarization independent absorption at Ku band frequencies." *Scientific Reports* 12(1): 20073.
- Bi, Y., et al. (2022). "Magnetically controllable holographic encryption based on a magneto-optical metasurface." *Optics Express* 30(5): 8366-8375.
- Chandra, M., et al. (2022). "A broadband transmissive type metasurface cross-polarization converter for EMC application." *IEEE Transactions on Electromagnetic Compatibility* 65(1): 186-194.
- Chandra, M., et al. (2022). "A broadband transmissive type metasurface cross-polarization converter for EMC application." *IEEE Transactions on Electromagnetic Compatibility* 65(1): 186-194.
- Cildir, A., et al. (2024). An Innovative Metasurface Polarizer Working in 5G Frequency Bands. 2024 18th European Conference on Antennas and Propagation (EuCAP), IEEE.
- Çıldır, A. (2024). "Multi-functional Multi-band Metasurface for Linear and Circular Polarization in Reflection Mode." *Teknik Bilimler Dergisi* 14(1): 26-30.
- Kamal, B., et al. (2021). "Design and experimental analysis of dual-band polarization converting metasurface." *IEEE Antennas Wireless Propagation Letters* 20(8): 1409-1413.
- Khan, M. I., et al. (2017). "Ultra-wideband cross polarization conversion metasurface insensitive to incidence angle." 121(4).
- Liu, J., et al. (2021). "Broadband polarization conversion metasurface for antenna RCS reduction." *Transactions on Antennas Propagation* 70(5): 3834-3839.
- Liu, J., et al. (2021). "Broadband polarization conversion metasurface for antenna RCS reduction." *IEEE Transactions on Antennas and Propagation* 70(5): 3834-3839.
- Liu, X., et al. (2022). "Dual-band dual-rotational-direction angular stable linear-to-circular polarization converter." *IEEE Transactions on Antennas and Propagation* 70(7): 6054-6059.
- Nasser, S. S. S. and Z. N. Chen (2021). "Low-profile broadband dual-polarization double-layer metasurface antenna for 2G/3G/LTE cellular base stations." *IEEE Transactions on Antennas Propagation* 70(1): 75-83.
- Qiu, L.-L., et al. (2023). "Wideband high-selective linear polarization converter and its application in bifunctional metasurface for reduced isolation band." 71(3): 2735-2744.
- Rashid, A., et al. (2023). "A single-layer, wideband and angularly stable metasurface based polarization converter for linear-to-linear cross-polarization conversion." *Plos one* 18(1): e0280469.
- Razzicchia, E., et al. (2023). *Metasurface Technology for Medical Imaging. Electromagnetic Imaging for a Novel Generation of Medical Devices: Fundamental Issues, Methodological Challenges and Practical Implementation*, Springer: 69-99.
- Samantaray, D. and S. Bhattacharyya (2020). "A gain-enhanced slotted patch antenna using metasurface as superstrate configuration." *IEEE Transactions on Antennas Propagation* 68(9): 6548-6556.
- Shah, S. M. Q. A., et al. (2021). "A multiband circular polarization selective metasurface for microwave applications." *Scientific reports* 11(1): 1774.
- Shukoor, M. A., et al. (2022). "Broadband chiral-type linear to linear reflecting polarizer with minimal bandwidth reduction at higher oblique angles for satellite applications." *IEEE Transactions on Antennas Propagation* 70(7): 5614-5622.
- Shukoor, M. A., et al. (2022). "Broadband chiral-type linear to linear reflecting polarizer with minimal bandwidth reduction at higher oblique angles for satellite applications." *IEEE Transactions on Antennas and Propagation* 70(7): 5614-5622.

- Ullah, N., et al. (2022). "Recent advancement in optical metasurface: fundament to application." *Micromachines* 13(7): 1025.
- Wahidi, M. S., et al. (2020). "Multifunctional single layer metasurface based on hexagonal split ring resonator." *IEEE access* 8: 28054-28063.
- Wang, K., et al. (2022). "Design of high-gain metasurface antenna based on characteristic mode analysis." *IEEE Antennas Wireless Propagation Letters* 21(4): 661-665.
- Wang, M. and Z. Zhai (2020). "Wide-angle circular polarization converter based on a metasurface of Z-shaped unit cells." *Frontiers in Physics* 8: 527394.
- Wu, X., et al. (2023). "Multitarget wireless power transfer system strategy based on metasurface-holography multifocal beams." *IEEE Transactions on Microwave Theory Techniques* 71(8): 3479-3489.
- Xu, G., et al. (2022). "Broadband polarization manipulation based on W-shaped metasurface." 9: 850020.
- Yang, H., et al. (2023). "A THz-OAM wireless communication system based on transmissive metasurface." *IEEE Transactions on Antennas Propagation* 71(5): 4194-4203.
- Zhang, X. G., et al. (2022). "A metasurface-based light-to-microwave transmitter for hybrid wireless communications." *Light: Science Applications* 11(1): 126.
- Zhao, Y., et al. (2019). "Ultra-wideband and wide-angle polarization rotator based on double W-shaped metasurface." *AIP Advances* 9(8).